04 Apr 1995, 2:30 pm - 3:30 pm

Critical Acceleration Levels for Free Standing Bridge Abutments

K. L. Fishman
State University of New York at Buffalo, NY

R. Richards Jr.
State University of New York at Buffalo, NY

R. C. Divito
State University of New York at Buffalo, NY

Proceedings: Third International Conference on Recent Advances in Geotechnical Earthquake Engineering and Soil Dynamics, April 2-7, 1995, Volume I, St. Louis, Missouri

Critical Acceleration Levels for Free Standing Bridge Abutments

Paper No. 2.12

K.L. Fishman, R. Richards, JR., and R.C. Divito
Assistant Professor, Professor and Graduate Student, Department of Civil Engineering, State University of N.Y. at Buffalo

SYNOPSIS: An analytic procedure for predicting threshold accelerations for movement of gravity wall bridge abutments due to earthquake loading is described. The method draws on previous work related to the sliding mode of failure, and a newly developed theory on seismic reduction of bearing capacity. The main contribution of this paper is to present laboratory observations verifying mode of failure and critical acceleration levels predicted by this procedure for model retaining wall bridge abutments subjected to seismic excitation on a shaking table. Three different test series were performed with different interface conditions between the wall, and the bridge deck, soil foundation, and backfill resulting in a variety of modes of wall deformation.

INTRODUCTION

Of the 40,000 bridge abutments in New York State almost all are free standing and more than half are founded on spread footings. Abutments founded on spread footings are not concentrated within one geographic locality but are distributed evenly throughout the various regions of the State (NYSDOT (1991), Younkins (1994)). If the inventory of bridge abutments in New York is considered typical of the Eastern United States the seismic vulnerability of free standing bridge abutments founded on spread footings is a major cause for concern, even with the moderate level of seismic risk associated with the Eastern U.S. region.

Richards and Elms (1979) introduced the displacement based approach for the seismic design of free standing, gravity wall type bridge abutments. Displacement based seismic analysis requires the determination of a threshold level of acceleration beyond which relative displacement between the gravity wall and foundation soil may occur. The original work by Richards and Elms (1979)considered only the possibility of a sliding mode of deformation. However, earthquake damage reports and laboratory tests indicate that wall failure by rotation is quite common.

Recent analytical studies address the possibility of a seismic reduction in bearing capacity beneath gravity retaining walls in which case, beyond a threshold acceleration level, a mixed sliding and/or rotation mode of deformation can result. Seismic bearing capacity is strongly dependent on the level of acceleration, the shear transfer between the wall footing and foundation soil, and the shear strength of the foundation soil. It will be shown that threshold levels of acceleration resulting in a loss of bearing capacity may be realized even for moderate earthquakes for retaining walls which are well designed from the standpoint of static loading.

In this study a general procedure for determining threshold acceleration levels for free standing gravity wall bridge abutments is developed. The procedure is comprehensive in that the seismic rotation of retaining walls can be considered in addition to the sliding mode of seismic wall movement. This is accomplished by investigating both a sliding failure mechanism, and the seismic reduction of bearing capacity at the base of the bridge abutment which induces rotation.

Although the ability to predict threshold acceleration levels for sliding has already been verified through experiments, there is a need to experimentally verify predictions of seismically induced bearing capacity failure. An important contribution of this paper is to present results from shake table testing of model gravity wall bridge abutments which fail by a coupled sliding/rotation mode. The tests described herein are an improvement over previous studies in the sense that the soil foundation beneath the abutment is included, and the model is not constrained to a tilting mode of failure but rather any possible mode of failure allowed.

THEORY

Fig. 1 shows the forces acting on a gravity wall bridge abutment during seismic loading. Loads from the bridge deck are considered to act at the top of the abutment. Depending on the connection detail, horizontal loads from the inertia of the

bridge deck may be transferred to the abutment. Body forces acting on the wall are present as well as lateral earth pressure behind the wall. It is also extremely important to consider the inertial loading applied to the foundation soil beneath the abutment footing.

Lateral earth pressures which develop behind rigid retaining walls which yield during earthquake loading may be evaluated using a rigid plastic model to describe soil behavior. The approach has been followed by Okabe (1926) and Mononobe and Matsuo (1929) who performed a modified Coulomb analysis in which the inertial load on the failed soil wedge was included in the analysis. The application of the Mononobe Okabe equation to seismic analysis of retaining walls is well established and details will not be repeated here. However, a relatively new approach to the problem of seismic reduction of bearing capacity is applied to the retaining wall problem and shall be described in what follows.

Seismic reduction in bearing capacity has been studied by Richards et al. (1990), and (1993), and Shi (1993). Seismic bearing capacity factors are developed considering shear tractions transferred to the soil surface as well as the effect of inertial loading on the wall and the soil in the failed region below the footing. For simplicity a "Coulomb-type" of failure mechanism is considered within the foundation consisting of an active wedge directly beneath the abutment and a passive wedge which provides lateral restraint with the angle of friction between them of $\phi/2$. Shi (1993) has verified this simple mechanism gives excellent results for the full range of soil properties by comparison to solutions using Sokolovski's method of characteristics. Bearing capacity is evaluated with a limit- equilibrium analysis whereby critical orientations of the failure planes are determined. Shear transfer between the footing and foundation soil is conveniently described by a friction factor:

$$f = \frac{S}{k_h F_v} \tag{1}$$

where S is the shear traction, k_h is coefficient of horizontal acceleration, and F_v is the normal force applied to the foundation.

The analytic solution gives a bearing capacity formula in terms of seismic bearing capacity factors N_{qE}, N_{cE}, $N_{\gamma E}$ as

$$q_{fE} = CN_{cE} + \gamma DN_{qE} + 1/2\gamma BN_{\gamma E} \tag{2}$$

similar to it's counterpart for the static case. For a surface footing on sand, only $N_{\gamma E}$ provides bearing capacity. Figure (2) presents the ratio of $N_{\gamma E}/N_{\gamma s}$, where $N_{\gamma s}$ is the static case bearing capacity factor, as a function of the friction angle of the foundation soil, ϕ, seismic acceleration coefficient, k_h, and f (Shi 1993).

Seismic Vulnerability

The seismic vulnerability of gravity wall bridge abutments involves the determination of a threshold acceleration beyond which permanent deformation of the gravity wall will occur. A thorough seismic analysis must investigate the possibility of both a sliding mode of failure as well as seismic reduction of bearing capacity introducing rotation. The analysis for the sliding failure mode is based on the theoretical and experimental work of Richards and Elms (1979), and has been well documented in the AASHTO (1992) code provisions and commentary. Seismic bearing capacity is a new development as applied to gravity wall bridge abutments and details of the analysis follow.

Since seismic bearing capacity factors are dependant on ground acceleration, determination of the threshold acceleration requires an iterative procedure easily programed for digital computation. Referring to Fig. 1:

(1) Assume a trial value for k_h and determine P_{AE} from the M-O equations.

(2) Compute the vertical force resultant, F_v, as

$$F_v = F_{DV} + P_{AE}\sin(\delta_w+\beta) + W_w \tag{3}$$

(3) Compute the resultant of the shear traction to be transferred to the foundation soil as

$$S = F_{DH} + P_{AE}\cos(\delta_w+\beta) + k_h W_w \tag{4}$$

(4) Compute the factor **f** using equation (1).

(5) Sliding will occur when $S = F_v\tan\delta_f$ and therefore

$$F.S._{slide} = \frac{\tan\delta_f}{k_h f} \tag{5}$$

where δ_f is the interface friction angle between the abutment footing and the foundation soil.

(6) Given the friction angle of the foundation soil, ϕ_f, and the "f" factor from step 4, find the seismic bearing capacity factor from figure (2).

(7) Compute the seismic bearing capacity q_{fE} using equation (2).

(8) Compute the ratio of the limit load to the actual load as

$$F.S._{B/C} = \frac{q_{fE}B_f}{F_v} \tag{6}$$

(9) If $F.S._{B/C}$ determined in step (8) is nearly equal to one and $F.S._{slide}$ from step (5) is greater than one, stop the iteration procedure. The assumed value for k_h is the threshold acceleration for bearing capacity failure, k_h^b.

(10) If $F.S._{slide}$ determined in step (5) is nearly

equal to one, and $F.S._{B/C}$ is greater than one, stop the iteration procedure. The assumed value for k_h is the threshold acceleration for sliding failure, k_h^s.

(11) If neither of the conditions in step (9) or (10) is met, select a new trial for k_h and return to step (1).

DESCRIPTION OF EXPERIMENTS

Model retaining walls were constructed in a seismic soil-structure interaction, test box. Details of the test box placed on the Shaking Table at the State University of New York at Buffalo and subjected to horizontal base acceleration are provided by Fishman, Mander and Richards (1994).

Ottawa sand (ASTM C-109) was used to study the response of dry sand in the test box. Engineering properties of this Ottawa sand are consistent and well established. Pluviation as described by Richards et al (1990) was used to place the soil in the test box. This placement method deposits a near homogeneous sand in a very dense state. In future testing, other densities may be obtained by varying the distance that sand is dropped from the hopper.

Model retaining walls, shown schematically in figure (3), were constructed having a height of 46 cm and a footing width between 15 and 20 cm. The foundation soil beneath the wall footing was 46 cm deep so that development of a failure region, necessary for seismic loss of bearing capacity, was not inhibited. The top of the model provided support for two (W8x10) girders representative of a bridge deck load. Although a prototype retaining wall may not be properly modeled in a 1 g test when elastic response is being considered, for the limit state scaling laws apply: i.e., if model dimensions are scaled in direct proportion to those of the prototype, forces on the prototype are proportional to the dimensional scaling factor squared and displacements are the same.

Three different models were tested. For Model I the bridge deck rested on a roller support such that no shear transfer was allowed between the deck and abutment. The abutment was designed such that a sliding mode of failure would likely occur. Model II used the same bridge deck/abutment connection detail, but failure from seismic loss in bearing capacity was anticipated. For Model III, a pinned connection between the bridge deck and abutment was used. Table 1 summarizes the parameters for each model including the wall weight, W_w, deck load, F_{deck}, width of footing, B_f, backfill/wall interface friction angle, δ_w, footing/foundation soil interface friction angle, δ_f, the soil friction angle, ϕ_f, unit weight of the backfill soil, γ_w, and unit weight of the foundation soil, γ_f.

Interface friction angles for Model I and Models II and III are different. In Model- I the interface was between smooth steel and sand. Models II and III were designed to reduce the risk of sliding failure. Interface shear strengths were increased by attaching coarse sand paper to the backside of the wall and the underside of the footing. Interface shear strengths were determined by pull tests with the model inside the test box.

Given the soil parameters and wall geometry for each model as presented in Table 1, static loading from active earth pressure P_{As}, and static safety factors against sliding and bearing capacity failure were computed as in Table 2. Table 3 summarizes the threshold acceleration levels computed for each model. These were determined using the analytic procedure already described. Dynamic active earth pressure, necessary to develop sliding failure, P_{AE}^s, or a bearing capacity failure, P_{AE}^b, are also shown in Table 3. The smallest of these values governs the seismic response of the wall.

Discussion of Results

Model walls were subjected to acceleration pulses and observations made to determine levels of threshold acceleration and mode of failure. Acceleration pulses were applied in increments of 0.05g through a range of 0.05g to 0.7g. At each level of acceleration the pulses were repeated three times.

Colored lines were placed in a horizontal and vertical grid pattern beneath the footing and behind the retaining wall to allow observation of the development of failure surfaces and soil deformations. Measurements at points indicated in Fig. 3 included relative displacements between the wall and the test box base, wall accelerations, backfill accelerations, and acceleration of the foundation soil.

Figure 4 displays the time history of relative horizontal and vertical displacement components for Model II. Permanent deformation is apparent at accelerations beyond the observed threshold value of 0.25 g. Characteristic of a bearing capacity failure, the measured vertical component of displacement is significant.

Acceleration measurements from Model II are shown in figure 5. These measurements were at an applied base acceleration beyond the predicted threshold for seismic loss of bearing capacity. A cutoff acceleration for the wall and backfill near the wall is clearly evident (comparing A16 and A8 to A7) indicating that soil within the failure region behind the wall has moved with the wall. Additionally, soil beneath the wall footing also exhibits a cutoff acceleration similar to that of the wall (comparing A16 and A13 to A6) . It may be concluded that as a result of seismic reduction of bearing capacity, the accelerometer beneath the wall footing is located in a failed region of soil and that this region of soil also displaces with the wall at accelerations beyond the threshold.

Subsequent to pulse testing model bridge abutments were subjected to acceleration time

functions which included cycles of loading, reverse loading and reloading. Both a ramped sine function and scaled record of the 1940 El Centro California earthquake were applied. Figures 6(a) and 6(b) show accelerations from the ramped sine function applied to the Model II bridge abutment and the resulting relative displacement. A wall cutoff acceleration close to 0.2g is evident. A comparison of displacement measurements from the top and near the base of the abutment indicates significant rotation of the abutment did occur when the computed threshold acceleration of $k_h^b = 0.22g$ was exceeded.

Summary of Results

Table 3 provides a summary of the observed threshold accelerations, k_h for the three models, and provides a comparison with thresholds predicted for sliding and bearing capacity, k_h^s and k_h^b. In all cases the observed threshold acceleration is close to the lowest, and therefore most critical predicted by the analysis for sliding and seismic reduction of bearing capacity modes. The comparison between predicted and observed threshold accelerations is good and implies a range of error between predicted and observed values of ± 0.05g.

CONCLUSIONS

The results presented in this paper demonstrate the strong possibility of seismic rotation of gravity wall bridge abutments in certain situations. This possibility exists even for cases where the static factor of safety against bearing capacity failure of the bridge abutment is in excess of 3.

The analytic method for predicting threshold accelerations for either a sliding or bearing capacity mode of failure has been verified through experiments. Model retaining walls were subjected to base accelerations via a shaking table and measurements of threshold accelerations were in close agreement with predictions. The laboratory models are general in the sense that a particular mode of failure was not forced, and a bearing capacity failure was allowed to take place beneath the abutment. A variety of wall deformation modes were studied by implementing different connection details between the abutment and bridge deck and also by varying the footing/foundation soil interface friction angle.

ACKNOWLEDGEMENT

This paper was prepared on the basis of research sponsored by the Federal Highway Administration (FHWA) and administered through the National Center for Earthquake Engineering Research (NCEER). The research reported herein is based on work conducted under Task 106-E-4.5 of FHWA Project DTFH61-92-C-00106, "Seismic Vulnerability of Existing Highway Construction."

DISCLAIMER

Any opinions, findings, conclusions, or recommendations expressed in this paper are strictly those of the authors and do not necessarily represent the views of the Federal Highway Administration, the National Center for Earthquake Engineering Research, or other participants in or sponsors of this work.

REFERENCES

1. AASHTO (1992). Guide Specifications for Seismic Design of Highway Bridges.

2. Fishman, K.L., Mander, J.B. and Richards, R. (1994). "Laboratory Study of Seismic Free Field Response of Sand", Soil Dynamics and Earthquake Engineering, Elsevier, to appear.

3. Mononobe, N. and Matsuo, H. (1929). "On the Determination of Earth Pressures During Earthquakes", Proc. World Engineering Congress, 9, 179-187.

4. NYDOT (1991). "Bridge Inventory Manual," Bridge Inventory and Inspection System, Albany, N.Y.

5. Okabe, S. (1926). "General Theory of Earth Pressure", J. Jap. Soc. of Civ. Eng., 12 (1).

6. Richards, R. and Elms, D. (1979). "Seismic Behavior of Gravity Retaining Walls", J. Geotech. Div., ASCE, 105 (4), 449-464.

7. Richards, R., Elms, D.G., and Budhu, M. (1990). "Dynamic Fluidization of Soils", Journal of Geotechnical Engineering, ASCE, 116(5), 740-759.

8. Richards, R., Elms, D.G., and Budhu, M. (1993). "Seismic Bearing Capacity and Settlements of Foundations", Journal of Geotechnical Engineering, ASCE, 119(4), 662-674.

9. Shi, X. (1993). "Plastic Analysis for Seismic Stress Fields", Ph.D. Thesis, State Univ. of N.Y., Buffalo, N.Y.

10. Younkins, J. (1994). "Seismic Vulnerability of Bridge Abutments in New York State", Master's Project, submitted to the Dept. of Civil Eng. State Univ. of N.Y. at Buffalo.

Table 1. Parameters for Model

Model	W_w (N)	F_{deck} (N)	B_f (mm)	ϕ_w	δ_w	δ_f	ϕ_f	γ_w kN/m^3	γ_f kN/m^3
I	276	818	143	30°	20°	20°	38°	15.4	17.0
II	1172	356	152	36°	22°	30°	38°	16.7	17.0
III	1221	356	203	36°	22°	30°	38°	16.7	17.0

Table 2. Static Factors of Safety

Model	P_{AS} (N)	FS_{slide}	$F.S._{BC}$
I[1]	347	1.4	1.4
II	374	2.77	3.7
III	374	2.86	3.54

(1) In Series I, H = 406 mm initially. H is 457 mm for models II and III.

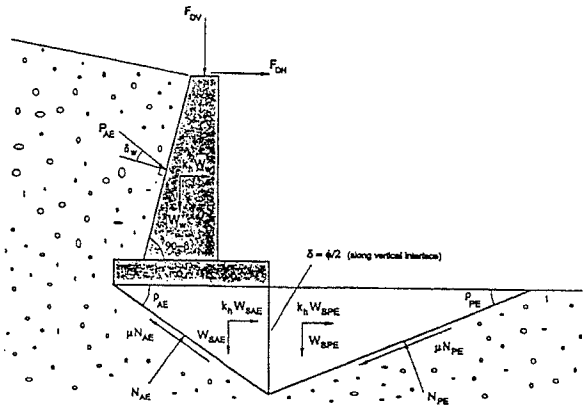

Figure 1. Forces Acting on a Gravity Wall Bridge Abutment During Seismic Loading.

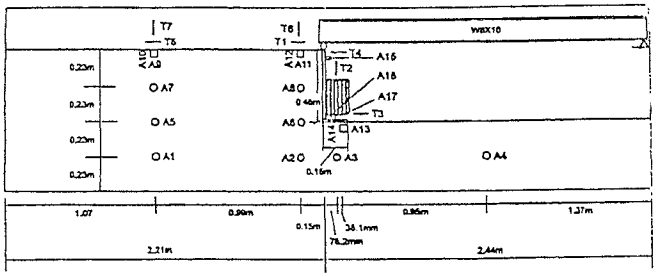

Figure 3. Schematic of Model Retaining Wall.

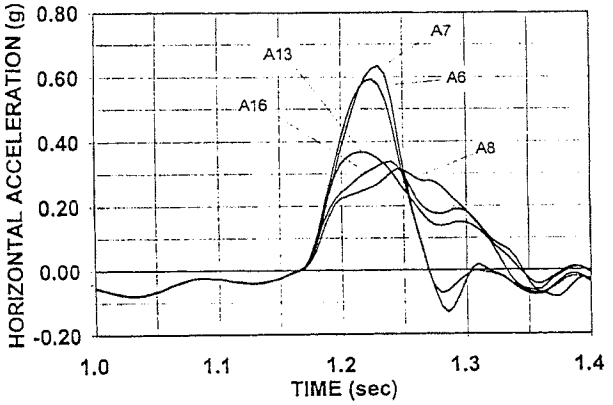

Figure 5. Wall Acceleration Compared to Backfill and Foundation Soil Acceleration for Model II.

Table 3. Threshold Levels of Acceleration

Model	P^a_{AE}/P^b_{AE} (N)	k^a_h (sliding)	k^b_h (bearing)	k^{obs}_h (observed)
I[1]	365/	0.2	0.5	0.25
II	743/587	0.30	0.22	0.25
III	1619/1023	0.60	0.43	0.35

(1) In Series I H = 356 mm when k_h = 0.2g. H is 457 mm for models II and III.

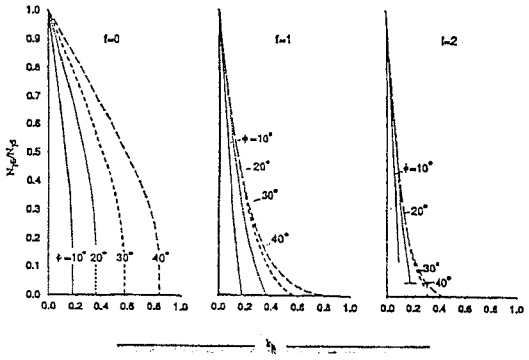

Figure 2. Ratio of Earthquake to Static Bearing Capacity Factor $N_{\gamma E}/N_{\gamma S}$.

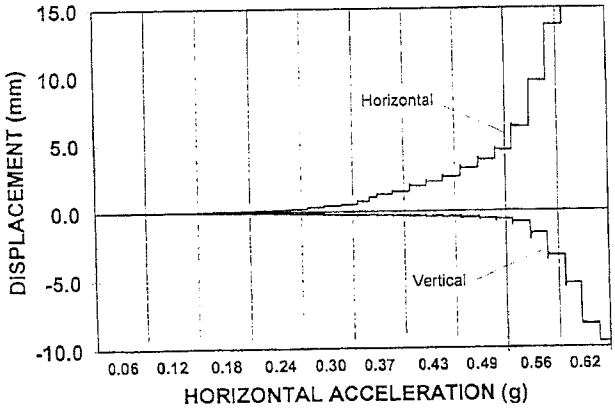

Figure 4. Time History of Relative Displacement for Model II.

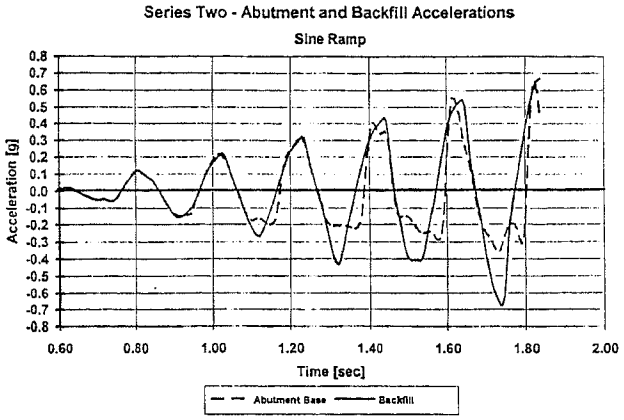

Figure 6a. Ramped Sine Acceleration Function Applied to Model II and the Resulting Wall Acceleration.

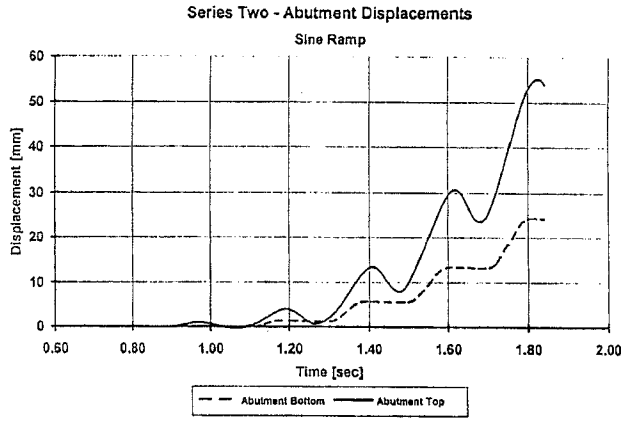

Figure 6(b) Time History of Relative Displacement for Model II in Response to Ramped Sine Function.